Unconventional Superconductivity in s-wave Superconductor-Magnet Heterostructure

A Thesis

Submitted to

Indian Institute of Science Education and Research Pune

in Partial Fulfilment of the Requirements
for the BS-MS Dual Degree Programme

by

Kartik Singh

Supervisor: Dr. Darshan G. Joshi

May 21, 2026

Certificate

This is to certify that this dissertation entitled "Unconventional Superconductivity in s-wave Superconductor-Magnet Heterostructure" towards the partial fulfilment of the BS-MS dual degree programme at the Indian Institute of Science Education and Research, Pune represents work carried out by Kartik Singh at TIFR Hyderabad under the supervision of Dr. Darshan G. Joshi during the academic year 2025-2026.

Dr. Darshan G. Joshi
Supervisor

Mr. Kartik Singh
Student

Committee:
Dr. Darshan G. Joshi
Dr. Sreejith G. J.

Declaration

I hereby declare that the matter embodied in the report entitled "Unconventional Superconductivity in s-wave Superconductor-Magnet Heterostructure" are the results of the work carried out by me at TIFR Hyderabad, under the supervision of Dr. Darshan G. Joshi and the same has not been submitted elsewhere for any other degree.

Dr. Darshan G. Joshi
Supervisor

Mr. Kartik Singh
Student

Statement of AI usage

No AI was used for producing this thesis.

This thesis is dedicated to everyone I love and cherish.

Acknowledgements

I would like to express my gratitude to my supervisor Dr. Darshan Joshi. My thesis progressed very smoothly because he always managed to find time and guide me. I am also grateful for his encouragement and guidance whenever I tried to pursue my interests and learn things outside of my project.

I would also like to thank Dr. Sreejith G. J., under whom I have previously worked. I found my current thesis project thanks to him. His advice and guidance have helped me multiple times. Without him, I wouldn't have made as much progress as I have.

I am greatly indebted to my parents and my younger brother. They have supported me on my journey far before I joined IISER Pune, and continue to do so. Even during tough times, they always made ends meet.

I cannot express how much I owe my friends, some of whom are halfway across the world. I can never forget all the ridiculous things Riya Bhandari got me into, the fuzzy thoughts Sujitha helped me figure out, the many late-night walks Ameya Kherde accompanied me on, the little panics Deepika Bhargava and I shared along, and the many, many trips, gossips, and mishaps I had with the Sus group. My 5 years at IISER Pune were a muse.

Last but not least, I would like to thank the people I met at TIFR. I want to thank Shivang Mathur for the interesting and stimulating discussions and for helping me with my PhD applications, and also Prithvi, Siddarth, Bharat, Shubhangi, and Anushree for showing me around Hyderabad and its cuisine.

List of Figures

List of Tables

Contents

Abstract

Much interest has gathered around topological superconductors, as it has been theorized that they can host exotic Majorana edge modes. These edge modes could serve as noise-resilient qubits in quantum computers, making them highly sought after. However, the experimental realization of topological superconductors has remained controversial. Some alternative methods have been proposed, one of which suggests that topological superconductivity can be induced by interactions with a magnetically ordered spin lattice.

In this thesis, we expand on this idea by considering the interface between an s-wave superconductor and a quantum paramagnet, called the spin ladder. We perform a careful analysis of this system, using diagrammatics and topological invariants, and search for any emergent topological superconductivity.

Chapter 1

Brief Overview of Topological Superconductors

Topological superconductors are highly sought-after phases of matter, as they can host exotic Majorana like excitations localized on the boundary [1]. These Majorana modes have found application as qubits for fault-tolerant quantum computers [2, 3, 4, 5, 6]. Even in theoretical research, Majorana modes have been the centre of interest as they are anyonic i.e., show neither fermionic nor bosonic statistics [4], and have connections to anomalies in high-energy physics [7].

Thus, much effort has been put into realizing topological superconductors (TSCs) and Majorana modes (MMs). However, the their existence still remains controversial [8, 9, 10, 11]. Alternate methods of realizing TSCs have been proposed, one of them being interfacing a normal s-wave superconductor (SC) with a spin lattice with magnetic order [12, 13, 14, 15]. In this work we build upon this idea and with a beyond mean-field analysis.

The outline of this chapter is as follows, in §1.1 we introduce p-wave TSC, and show how it manifests Majorana modes. In §1.2 we take a tangent to discuss the role of topology in condensed matter physics. Then, with heuristic arguments, we explain that the robustness of MMs is a topological feature. We end the section with some results from topological band theory. At the end of the chapter in §1.3, we will mention some literature on superconductor-magnet interfaces.

1.1 p-Wave superconductors

One of the simplest examples of TSC in 1D is the p-wave superconductor. In a p-wave SC, the gap function is odd w.r.t inversion of momenta and the attractive interaction encourages triplet pairings i.e., electrons of the same spin. The simplest toy hamiltonian that has these features is the Kitaev chain [1],

$$H = \mu \sum_{x,\alpha} c^\dagger_{x,\alpha} c_{x,\alpha} + \sum_{x,\alpha} \left(\frac{t}{2} c^\dagger_{x,\alpha} c_{x+1,\alpha} + \Delta c^\dagger_{x,\alpha} c^\dagger_{x+1,\alpha} + \text{h.c.} \right) \tag{1.1}$$

where, c_x is the electron annihilation operator at site x.

Any spin-1/2 Dirac fermion can be broken into two Majorana fermions. Moreover, a Majorana fermion is its own antiparticle, so the creation (annihilation) operators must satisfy, $\gamma^\dagger = \gamma$. Under these conditions, the Majorana operator basis is defined as,

$$\gamma_{x,A} = c^\dagger_x + c_x, \quad \gamma_{x,B} = i(c^\dagger_x - c_x)$$

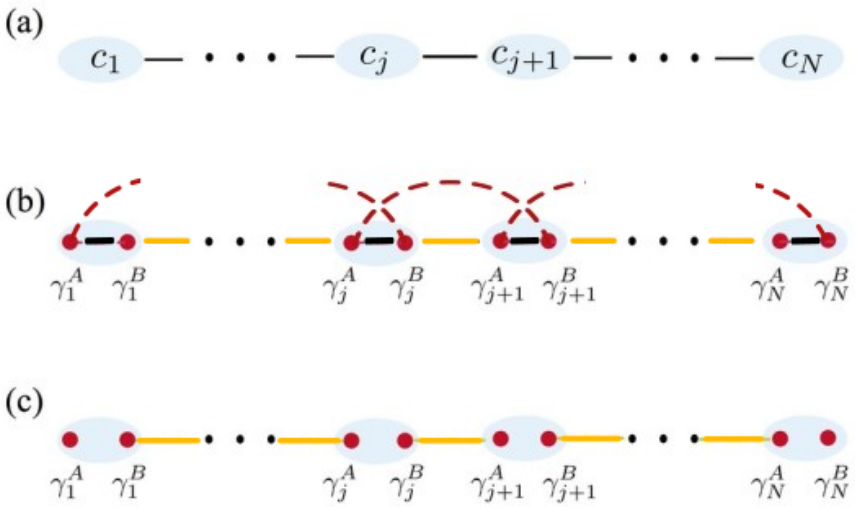

Figure 1.1: Kitaev chain. (a) Schematic of the model in electron basis, the lines depict which pairs are coupled. (b) Each electron can be decomposed into two Majoranas. Red and orange line depict $t_\pm$ coupling, whereas black decipts μ coupling. (c) Setting $t = |\Delta|$ and $\mu = 0$ only leaves the t_+ coupling, therefore decoupling the Majorana operators on the ends.

the hamiltonian in Eq.(1.1) when re-written in Majorana basis takes the form,

$$H = -\frac{i\mu}{2}\sum_{x=1}^{N}\gamma_{x,B}\gamma_{x,A} + \frac{i}{2}\sum_{x=1}^{N-1}\left(t_+\gamma_{x,B}\gamma_{x+1,A} + t_-\gamma_{x+1,B}\gamma_{x,A}\right) \tag{1.2}$$

where $t_\pm = |\Delta| \pm t$.

It's worth mentioning that topological insulators also have boundary states, but they aren't Majorana like. This is because $c^\dagger c$ terms always produces Majorana operators in pair, but the $c^\dagger c^\dagger$ term makes it possible to isolate a Majorana excitation. We can do this in Eq.(1.2) by setting $t = |\Delta|$ and $\mu = 0$,

$$H = i\Delta\sum_{x=1}^{N-1}\gamma_{x,B}\gamma_{x+1,A}. \tag{1.3}$$

Notice $\gamma_{1,A}$ and $\gamma_{n,B}$ are decoupled, see Fig.1.1. Thus $\gamma_{1,A}|0\rangle$ and $\gamma_{n,B}|0\rangle$ are eigenstates, and these are precisely the edge-localized Majorana modes we were looking for.

In fact, for $\mu \leqslant |t|$ there are still MMs. In this regime, the Kitaev chain becomes a TSC, for exact definition see §1.2.1. Away from $\mu = \pm|t|$, the MMs develop a tail that decays as $e^{\pm\lambda x}$ into the bulk. As long as the Majoranas are separated by a distance larger than λ, we can make use of their exotic anyonic properties.

Robustness of Majorana modes To reasonably realize and use Majoranas, we need to make sure that these states survive against weak disorder. As it turns out, certain edge states are a feature of the topology of the Bloch states, this is a corollary of the Bulk-boundary correspondence (BBC). Any weak disorder due to impurity may deform the Majorana states, but never fully destroys them.

As stated earlier, in the next section, we won't rigorously prove the BBC or the robustness of MMs, but merely provide heuristic arguments to support it.

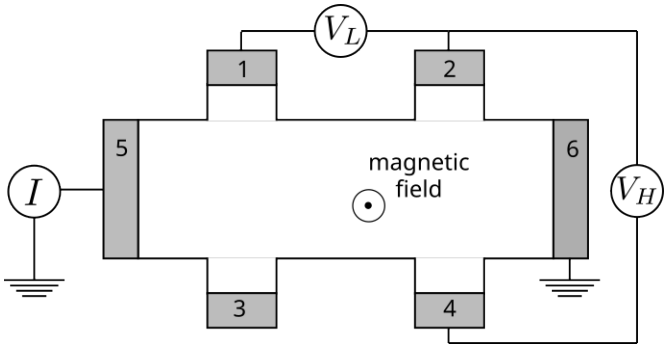

Figure 1.2: Quantum Hall circuit diagram.
Souce: topcondmat.org

1.2 Topology in condensed matter physics

The most well-known example of effect of topology in condensed matter systems is the Quantum Hall effect (QHE) in 2D materials [16]. When a current I is applied through a metal strip in the presence of a magnetic field, a transverse voltage V_H develops in the metal, see Fig.1.2. In other words, the hall conductance $\sigma_{xy} = I/V_H$, is non-zero. QHE refers to the quantization of hall conductance, given by $\sigma_{xy} = ne^2/h$, where $n \in \mathbb{I}$.

Certain features of QHE were especially puzzling. Firstly, the phenomenon was quite robust, being independent of proportions of the sample, electron density and impurities. Modern experiments show deviations $\leqslant 1$ part in 10^{10} [17]. Secondly, in the regime where σ_{xy} is non-zero, the bulk is an insulator, see Fig.1.3. It wasn't clear what was allowing the transport of electrons from one end to the other.

TKNN formula This formula was proposed by Thouless et al. in their work [19], in an attempt to explain the quantized hall conductance in QHE. The expression they derived is as follows,

$$\sigma_{xy} = \frac{e^2}{2\pi\hbar}\sum_{\alpha} C_\alpha$$

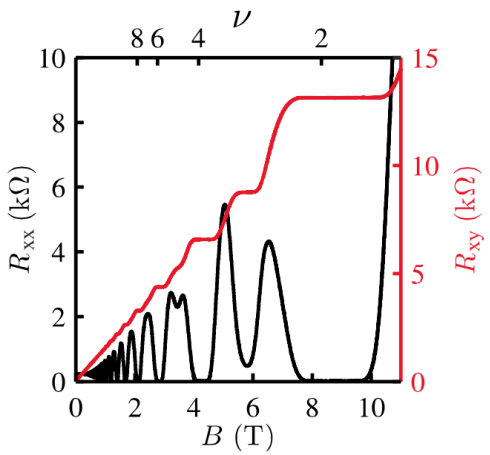

Figure 1.3: Quantization of hall conductance. R_{xy} and R_{xx} are the transverse and longitudinal resistances, respectively. These are measured indirectly via capacitance microscopy, thus the vanishing R_{xx}, really means $\to \infty$ resistance
Souce: Suddards et. al. [18]

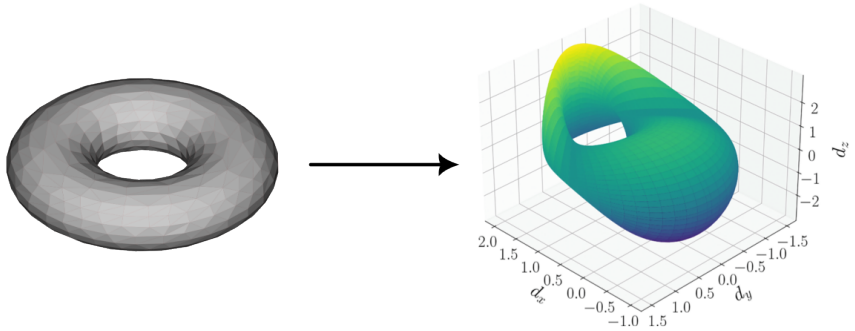

Figure 1.4: Representation of chern number.

where, α sums over occupied bands, C_α is the chern number of α band. The chern number is defined as,

$$C_\alpha = \frac{i}{2\pi}\int_{\mathrm{BZ}} d^2\mathbf{k}\,\Omega(\mathbf{k}), \quad \Omega(\mathbf{k}) = \langle \partial_x u^\alpha_{\mathbf{k}} | \partial_y u^\alpha_{\mathbf{k}} \rangle - \langle \partial_y u^\alpha_{\mathbf{k}} | \partial_x u^\alpha_{\mathbf{k}} \rangle$$

Chern number as topological invariant To explain the properties of chern number, we consider a general 2-level system in 2D. A generic 2-level Hamiltonian is given by,

$$H(\mathbf{k}) = d_x(\mathbf{k})\sigma_x + d_y(\mathbf{k})\sigma_y + d_x(\mathbf{k})\sigma_z$$

Using this, we can define a map that takes $\mathbf{k}$ to $\mathbf{d} = (d_x, d_y, d_z)$. Fig.1.4, provides a visual for this mapping. Due to periodicity, the 2D Brillouin zone (BZ) is a torus. Therefore, this map embeds the BZ (torus) into a 3D vector space. The chern number computes the number of times the image of BZ (torus) wraps around the origin. With this interpretation, we can say the chern number,

- is always an integer i.e, it is quantized
- only changes if the image of BZ crosses origin. Only possible if $d(k) = 0$ for some $\mathbf{k}$ i.e., the two bands must touch somewhere. Recall, in a Kitaev chain the transition between SC and TSC phase is marked by $\mu = \pm|t|$, which is exactly where its band gap closes.
- only depends on the overall shape of the image of BZ, and not any local details of $d(\mathbf{k})$. It's a **topological invariant.**

The argument we presented can be generalised to higher dimensions. These are general properties of not just chern number, but of topological invariants.

These properties explain both the quantization and robustness of hall conductance. Random perturbations that are too weak to close the bulk gap can't change the chern number and consequently, neither the hall conductance.

Protected edge modes Now we can present the argument for BBC. Say two materials A and B with different values of chern number are joined at their boundary. Without the loss of generality, we assume the boundary lies along $y = 0$, in $y < 0$ is material A and

$y > 0$ is material B. Also, let H_A and H_B be the hamiltonian describing material A and B, respectively.

The total hamiltonian of the system can be modelled using,

$$H = g(-y)H_A + g(y)H_B\,, \quad g(y) \sim (e^{-ay}+1)^{-1}$$

the idea is that $g(y)$, would behave like a boundary potential. Now, say we begin from deep inside H_A, and start moving towards positive y. $g(y)H_B$ can be thought of a potential begin turned on with "time" y.

Somewhere near the crossing $y = 0$, we expect a transition from phase of H_A to H_B. Now, because A and B have different chern numbers, this transition cannot occur without gap closing in H. The only parameter being varied is y, thus for some y_0, the bands of H collapse into a flat band along the entire line $y = y_0$.

Finally, set $a \to \infty \Rightarrow y_0 = 0$ and choose B to be vaccum (0 chern number). The flat bands allow delocalized states to propagate along the entire $y = 0$ line, essentially edge modes. Thus, any material having non-trivial chern number guarantees edge modes at the boundary of the material. Moreover, since weak perturbations can't change topological invariants, they also can't destroy edge modes.

1.2.1 Results from topological band theory

One of the main ideas of topological band theory is to use topological invariants to classify phases of matter. Labelling states with different invariants as distinct phases is justified. The reason is, topological invariants are related to physical observables, like the hall conductance as shown by TKNN. Moreover, topological invariants make good labels as they are quantized.

This scheme is completely different from Landau theory, wherein classification is based on order parameters and symmetries. A phase (or material like SC) is said to be topological if any of the topological invariants are non-trivial. Now we summarize the two main results from topological band theory that we will use in this work,

AZ classification This is an exhaustive topological classification of non-interacting fermionic systems on the basis of the symmetries of the hamiltonian. First, Altland and Zirnbauer showed that all free fermionic hamiltonians can be classified using three symmetries, namely time reversal symmetry (TRS), particle-hole symmetry (PHS), and chiral symmetry (CS) [20]. Say the hamiltonian is written in the lattice basis,

$$H = \sum \psi^\dagger_{i\alpha} h_{i,\alpha\beta}\, \psi_{i\beta}$$

where h_i is the single particle hamiltonian matrix, and ψ_i is a spinor at site i. The symmetries can be represented as unitary matrices of the following type,

$$\begin{array}{ll} \text{TRS}: & h = T h^T T^{-1}, \quad T^T = \alpha T \\ \text{PHS}: & h = -P h^T P^{-1}, \quad P^T = \beta P \\ \text{CS}: & h = -C h^T C^{-1}, \quad C^2 = \mathbb{I} \end{array} \,. \tag{1.4}$$

Later, Shinsei Ryu et. al. worked out the possible topological phases that can exist in each symmetry class, and also their corresponding topological invariants [21, 22]. The results are summarized in Table.1.1.

Class	TRS	PHS	CS	$d=1$	$d=2$	$d=3$	$d=4$
A	0	0	0	0	$\mathbb{Z}$	0	$\mathbb{Z}$
AIII	0	0	1	$\mathbb{Z}$	0	$\mathbb{Z}$	0
AI	+1	0	0	0	0	0	$\mathbb{Z}$
CI	+1	-1	1	0	0	$\mathbb{Z}$	0
BDI	+1	+1	1	$\mathbb{Z}$	0	0	0
AII	-1	0	0	0	$\mathbb{Z}_2$	$\mathbb{Z}_2$	$\mathbb{Z}$
CII	-1	-1	1	$\mathbb{Z}$	0	$\mathbb{Z}_2$	$\mathbb{Z}_2$
DIII	-1	+1	1	$\mathbb{Z}_2$	$\mathbb{Z}_2$	$\mathbb{Z}$	0
C	0	-1	0	0	$\mathbb{Z}$	0	$\mathbb{Z}_2$
D	0	+1	0	$\mathbb{Z}_2$	$\mathbb{Z}$	0	0

Table 1.1: Altland-Zirnbauer classification

In the table, d denotes the spatial dimension of the system. 2^{nd} and 3^{rd} columns denote the value of α and β, respectively. If a symmetry doesn't exist it is denoted by 0. The latter columns tell whether the particular combination of symmetries and spatial dimensions allows non-trivial topological phases. Here, 0 denotes that the topology is always trivial, $\mathbb{Z}$ and $\mathbb{Z}_2$ denote that a non-trivial chern number or $\mathbb{Z}_2$ invariant is possible.

Bulk-boundary correspondence The full version of BBC doesn't just garuntee the existence of edge states, but also relates topological invariants to the type and number of edge modes. We will merely state the result in 1D, as it is the most relevant to us,

- The winding number (chern number in 1D) equals the number of end states.
- $\mathbb{Z}_2$ is the number of kramer doublets crossing the fermi surface.

1.2.2 Interaction induced topology

There are many challenges in extending the AZ classification to interacting systems, such as the fact that the Brillouin zone is not defined, and the lack of exactly solvable models. There is some literature, like classification of interacting systems with time-reversal symmetry [23, 24]. While these studies are not exhaustive, they do show that interactions can change the topology of a system.

Largely, the topology of interacting systems is studied using perturbative methods. The assumption is that if the system is gapped and interactions are not too strong, then the interacting and non-interacting states can be adiabatically connected. What's of interest to us is whether interactions can turn a trivial superconductor into a topological one?

1.3 Superconductor-magnet interfaces

As stated at the beginning of chapter, there hasn't been a confirmed realization fo TSC. The conventional approach is to use Rashba-spin orbit (RSO) coupling to induce a triplet pairing of electrons, which could potentially induce a p-wave gap like in the Kitaev chain. Challenges with this method are 1) materials where RSO has a dominant

triplet pairing are hard to find, and 2) RSO depends mostly on the overlap of atomic orbitals, and thus offers limited tunability.

The above difficulties can be avoided if topology is induced solely through external influence. Beenakker et. al. [13] showed that a spatially varying magnetic field can give rise to MMS in a normal SC. Later, Nagaosa et. al. [15] found that coupling an s-wave SC to a helical or skyrmionic spin lattice, induced $p_x + p_y$ and $p_x + ip_y$ like pairing. Finally, Schnyder et. al. [12] found that this phenomenon occurs in a wide range of magnetically ordered materials. They even found $p_r + ip_\phi$-wave like pairing.

All the above mentioned works use first-order mean-field analysis i.e., spins in the lattice are considered to be frozen. Moreover, their spin lattices are magnetically ordered. In this thesis, we expand on this idea by analyzing one such SC-magnet interface. We ask if topological superconductivity can be induced without an overall magnetic order, solely through the dynamics of another system. In the next chapter, we introduce the magnetic system we chose for this work.

Chapter 2

Topological Quantum Paramagnets

In this chapter, we introduce the magnetic system that is of interest to us. Loosely speaking, we are looking to "transfer" topological features from a magnetic lattice into a trivial superconductor. Therefore, we would want to pick a magnetic system that has non-trivial topological phases. A good place to look at is the subclass of systems called Quantum paramagnets. These systems are gapped, and thus corrections due to SC will be comparatively small. They also have no magnetic order as desired.

The spin-ladder is one of the simplest 1D quantum paramagnets that show non-trivial topological phases, making it well-suited for our purposes. In this chapter, we will introduce the analytical method used to study spin-ladder i.e., the triplon bond operators. We will conclude by mentioning the features of the topological phase of the spin ladder.

2.1 Spin-ladder

The spin-ladder is constructed by taking two 1D Heisenberg spin-1/2 chains parallel to each other, as shown in Fig.2.1. The spins in the top chain $S_{1,i}$ are coupled to the spins in the bottom chain $S_{2,i}$ via another Heisenberg interaction. Thus, giving it the shape of a ladder. The hamiltonian is as follows,

$$H_{\mathrm{SL}} = \sum_i \Big(J\mathbf{S}_{1i} \cdot \mathbf{S}_{2i} + J'(\mathbf{S}_{ri} \cdot \mathbf{S}_{ri+1}) \Big)$$

For $|J| \gg |J'|$ and $J > 0$, the ground state must have every $(S_{1,i}, S_{2,i})$ pair in singlet. In this limit, the spin ladder can be thought of as a 1D Heisenberg chain of dimers. The excitations are formed by breaking the singlet dimers in the ground state into triplet states.

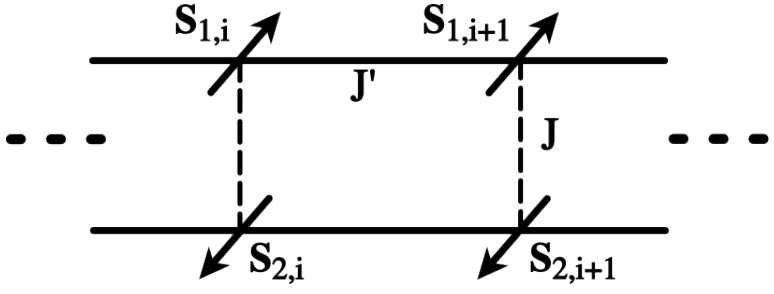

Figure 2.1: The spin ladder model

Before we talk about the dynamics of these triplet states, in order to see a topological phase, we need to add some extra ingredients to the above model.

$$H_{\mathrm{SL}} = \sum_i \Big(J\mathbf{S}_{1i}\cdot\mathbf{S}_{2i} + J'(\mathbf{S}_{ri}\cdot\mathbf{S}_{ri+1}) + D(S^z_{ri}S^x_{ri+1} - S^x_{ri}S^z_{ri+1}) + \\ + \Gamma(S^z_{ri}S^x_{ri+1} + S^x_{ri}S^z_{ri+1}) + h_y(S^y_{1i} + S^y_{2i}) \Big) \tag{2.1}$$

the D and Γ are anisotropic spin interactions, which come from relativistic effects called the Dzyaloshinskii-Moriya (DM) interactions. Along with these, we also introduce a magnetic field in the y-direction. Next, we use the triplon-bond operator formalism to analyze the dynamics of the excitations i.e., triplet states.

2.1.1 Triplon-bond operator formalism

First, we introduce the following shorthand notation for the state of spins in the dimer pair at site i,

$$\begin{aligned}
|t_{i0}\rangle &= \tfrac{1}{\sqrt{2}}(|\uparrow\rangle_{i,1}|\downarrow\rangle_{i,2} - |\downarrow\rangle_{i,1}|\uparrow\rangle_{i,2}) \\
|t_{ix}\rangle &= \tfrac{-1}{\sqrt{2}}(|\uparrow\rangle_{i,1}|\uparrow\rangle_{i,2} - |\downarrow\rangle_{i,1}|\downarrow\rangle_{i,2}) \\
|t_{iy}\rangle &= \tfrac{i}{\sqrt{2}}(|\uparrow\rangle_{i,1}|\uparrow\rangle_{i,2} + |\downarrow\rangle_{i,1}|\downarrow\rangle_{i,2}) \\
|t_{iz}\rangle &= \tfrac{1}{\sqrt{2}}(|\uparrow\rangle_{i,1}|\downarrow\rangle_{i,2} + |\downarrow\rangle_{i,1}|\uparrow\rangle_{i,2})
\end{aligned}$$

The triplon operators $t^\dagger_{i\gamma}$ change the state of dimer at site i, from a singlet to triplet γ i.e., $t^\dagger_{i\gamma}|t_{i0}\rangle = |t_{i\gamma}\rangle$ and also $t_{i\gamma}|t_{i\gamma}\rangle = |t_{i0}\rangle$.

To make sure the triplon operators faithfully represent the dynamics, we need a way to ensure that the number of triplons at any site shouldn't exceed one. One way to implement this is to use projection operators, $P_i = 1 - t_{i\alpha}t_{i\alpha}$ [25]. With all this, the spin operators can be written in terms of triplet operators as follows,

$$S^\alpha_{1,2i} = \frac{1}{2}\left(\pm i t^\dagger_{i\alpha} P_i \mp P_i i t_{i\alpha} - i\varepsilon_{\alpha\beta\gamma} t^\dagger_{i\beta} t_{i\gamma} \right);$$

We adopt the the convention of multiplying by i, used in [26, 27], to preserve the behaviour of the spin operator under time reversal.

2.1.2 Effective triplon hamiltonian

We are only interested in the low-energy dynamics of the spin-ladder i.e., excitations with the total triplon number being one. A low-energy description is enough for two reasons. Firstly, past literature has shown that the first band has non-trivial topology [27]. Secondly, there will be a significant band gap between 2$^{\text{nd}}$ and 1$^{\text{st}}$ excited state due to $|J| \gg |J'|$. Therefore, the corrections to the SC from 2$^{\text{nd}}$ or higher excited states will be suppressed.

We also make the harmonic approximation, wherein we neglect terms higher than 2$^{\text{nd}}$ order in triplons. Surprisingly, we don't lose out much. This approx. decouples the t_y mode from t_x, t_z mode. The effective hamiltonian of the t_x, t_z space is,

$$H_k = \frac{1}{2}\sum_k \Psi^\dagger_k h(k) \Psi_k,$$

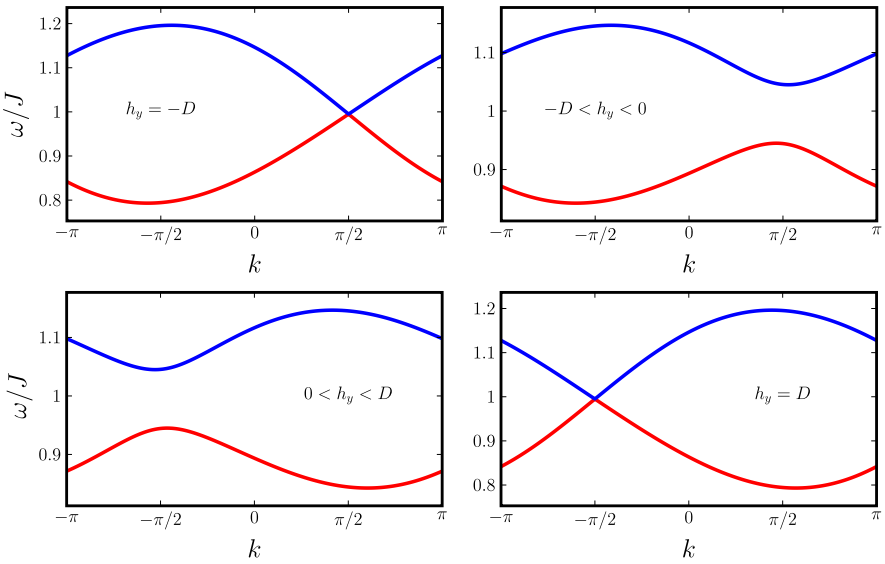

Figure 2.2: Spectrum of t_x and t_z triplon bands
Souce: D. Joshi, A. P. Schnyder [27]

with the spinor $\Psi_k = (t_{kx}, t_{kz}, t^{\dagger}_{-kx}, t^{\dagger}_{-kz})^T$ and matrix,

$$h(k) = \begin{pmatrix} h_1(k) & h_2(k) \\ h_2^{\dagger}(k) & h_1^T(-k) \end{pmatrix}; \quad \begin{matrix} h_1(k) = (J + J'\cos(k))\mathbb{I} + \mathbf{d}\cdot\sigma; \\ h_2(k) = -J'e^{-ik}\mathbb{I} - \mathbf{x}\cdot\sigma \end{matrix} \tag{2.2}$$

where $\mathbf{d} = \{\Gamma\cos(k), -D\sin(k) - h_y, 0\}$ and $\mathbf{x} = \{\Gamma\cos(k), -D\sin(k), 0\}$. The spectrum computed from the above hamiltonian is shown in Fig.2.2. It shows band gap closing at paramater values $h_y = \pm D$, for $D = \Gamma$, giving the possibility of a topological phase transition.

2.1.3 Topological invariant and end states

In this section, we briefly summarize the procedure in [27] on how the topological phase of the spin ladder is characterised.

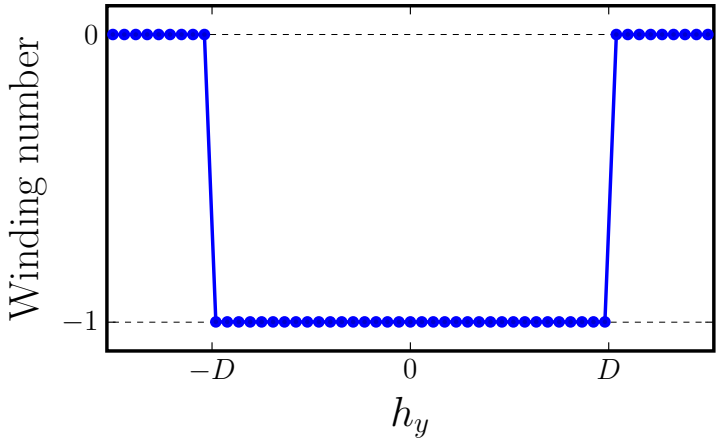

Figure 2.3: Winding number of t_x and t_z triplon bands
Souce: D. Joshi, A. P. Schnyder [27]

First we find a unitary transform U that will get $\Sigma h(k)$ in a block-diagonal form, where $\Sigma = \text{Diag}(\mathbb{I}, -\mathbb{I})$

$$U\Sigma h(k)U^\dagger = \begin{pmatrix} A(k) & D_1(k) \\ D_2(k) & A(k) \end{pmatrix}$$

then we compute the following quantity,

$$\nu = \frac{1}{2}\frac{1}{4\pi i}\int_{BZ} dk\, Tr\left[D_k^{-1}\partial_k D_k - (D_k^\dagger)^{-1}\partial_k D_k^\dagger\right] \tag{2.3}$$

where, $D_k = (D_1(k) + D_2^\dagger(k))/2$.

The quantity ν is a topological invariant that, in this case, captures the winding number of the triplon bands. The change in ν coincides with the band gap closing in parameter space, see Fig.2.3. Therefore, by bulk-boundary correspondence, there should be end states in the spin-ladder for $-D \leqslant h_y \leqslant D$. A few key features of these end states worth noting are:

- These end states are localized at the 2 ends of the spin-ladder, with total triplon number being 1. Thus, we have half a triplon at each end.
- These end states aren't zero-energy modes. Being made of triplons, these end states have a finite energy.

2.2 Alternate model

There is another set of parameters for which the spin ladder shows topological end-states. To get to this, one has to change the "orientation" of the Γ interaction. Rather than anti-symmetically coupling S^x and S^z on neighbouring sites, we couple S^x and S^y.

$$\begin{aligned} H_{\text{SL}} = \sum_i \Big(& J\mathbf{S}_{1i}\cdot\mathbf{S}_{2i} + J'(\mathbf{S}_{ri}\cdot\mathbf{S}_{ri+1}) + D(S^z_{ri}S^x_{ri+1} - S^x_{ri}S^z_{ri+1}) + \\ & + \Gamma(S^y_{ri}S^x_{ri+1} + S^x_{ri}S^y_{ri+1}) + h_y(S^y_{1i} + S^y_{2i})\Big) \end{aligned} \tag{2.4}$$

In this case, there is no decoupling, all three triplon modes mix with each other. The hamiltonian in this setting is given by,

$$H = \frac{1}{2}\sum_k \Psi_k^\dagger h(k)\Psi_k,$$

where, $\Psi_k = (t_{kx}, t_{ky}, t_{kz}, t^\dagger_{-kx}, t^\dagger_{-ky}, t^\dagger_{-kz})^T$ and the matrix

$$h(k) = \begin{pmatrix} h_1(k) & h_2(k) \\ h_2^\dagger(k) & h_1^T(-k) \end{pmatrix}; \quad \begin{aligned} h_1(k) &= (J + J'\cos(k))\mathbb{I} + \mathbf{d}\cdot\mathbf{L}; \\ h_2(k) &= -J'e^{-ik}\mathbb{I} - \mathbf{x}\cdot\mathbf{L} \end{aligned} \tag{2.5}$$

where,

$$\mathbf{L} = \left\{ \begin{bmatrix} 0 & 1 & 0 \\ 1 & 0 & 0 \\ 0 & 0 & 0 \end{bmatrix}, \begin{bmatrix} 0 & 0 & -i \\ 0 & 0 & 0 \\ i & 0 & 0 \end{bmatrix}, \begin{bmatrix} 0 & 0 & 0 \\ 0 & 0 & 1 \\ 0 & 1 & 0 \end{bmatrix} \right\}$$

$$\mathbf{d} = \{\Gamma\cos(k), -D\sin(k) - h_y, 0\}$$
$$\mathbf{x} = \{\Gamma\cos(k), -D\sin(k), 0\}$$

The computation of winding number isn't straightforward, and we won't show it here, the details are in [27]. Regardless, the model still shows a topological phase for $-D < h_y < D$, that has triplon end-states. Another difference is that the end-states in this case are dispersive.

This concludes our discussion of the spin ladder. We have seen that it's a relatively simple model that shows topological features for a variety of parameters. As planned, in the next chapter, we will see if these topological features can be passed onto an s-wave superconductor.

Chapter 3

Interaction-induced Unconventional Superconductivity

In this chapter, we finally study the effects on the s-wave SC when interfaced with the spin-ladder. The most common interaction induced by interfacing is the Kondo interaction, which is what we use to couple the superconductor with the spin-ladder.

There are two major parts of our analysis. First is computing the corrections to the s-wave Cooper pairs due to Kondo coupling, which we discuss in §3.2. For this part, we use the Feynman diagrammatic expansion. Second, we need to find the topological invariant that characterizes the interacting SC. Here, we introduce the analytical tool used for this purpose called the topological hamiltonian, which will be the point of discussion in §3.3.

3.1 Superconductor spin-ladder interface

We assume that the 1D BCS lattice only couples to the top layer of the spin-ladder via Kondo coupling. The full hamiltonian is as follows,

$$H = H_{\text{BCS}} + H_{\text{SL}} + H_{\text{int}} \tag{3.1}$$

$$H_{\text{BCS}} = \sum_k \left(\xi_k c^\dagger_{k\alpha} c_{k\alpha} - \left(\Delta_k c^\dagger_{k\uparrow} c^\dagger_{-k\downarrow} + \text{h.c.} \right) \right) \tag{3.2}$$

$$H_{\text{int}} = J_K \sum_i \left(\mathbf{S}_{1,i} \cdot \sigma_{\alpha\beta}\ c^\dagger_{i\alpha} c_{i\beta} \right) \tag{3.3}$$

where, $\xi_k = \cos(k) + \mu$, and H_{SL} is the spin-ladder hamiltonian from Eq.(2.1). We use the same procedure used in the analysis of the spin-ladder. First we re-write the $\mathbf{S}_i$ in kondo term using triplon operators,

$$\begin{aligned} \mathbf{S}_{1,i} \cdot \sigma_{\alpha\beta}\ c^\dagger_{i\alpha} c_{i\beta} = \Big\{ & \Big((t^\dagger_{iy} + i t^\dagger_{ix}) P - P(t_{iy} + i t_{ix}) \\ & + t^\dagger_{ix} t_{iz} - t^\dagger_{iz} t_{ix} + i t^\dagger_{iz} t_{iy} - i t^\dagger_{iy} t_{iz} \Big) c^\dagger_{i\uparrow} c_{i\downarrow} + \text{h.c.} \Big\} \\ & + \left(i t^\dagger_{iz} P - P i t_{iz} + i t^\dagger_{iy} t_{ix} - i t^\dagger_{ix} t_{iy} \right) \left(c^\dagger_{i\uparrow} c_{i\uparrow} - c^\dagger_{i\downarrow} c_{i\downarrow} \right), \end{aligned}$$

we also keep the harmonic approx. and ignore boson terms above 3[rd] order. Converting to fourier basis we get,

$$\begin{aligned} J_K^{-1} H_{\text{int}} = \delta_{q'-q+k'-k} \Big\{ \Big((t^\dagger_{q'y} + i t^\dagger_{q'x})(\delta_q - i t_{qz}) + (i t^\dagger_{q'z} - \delta_{q'})(t_{qy} + i t_{qx}) \Big) c^\dagger_{k'\uparrow} c_{k\downarrow} + \text{h.c.} \Big\} \\ + \delta_{q'-q+k'-k} \Big((i t^\dagger_{q'z} \delta_q - i t_{qz} \delta_{q'}) + i t^\dagger_{q'y} t_{qx} - i t^\dagger_{q'x} t_{qy} \Big) \Big(c^\dagger_{k'\uparrow} c_{k\uparrow} - c^\dagger_{k'\downarrow} c_{k\downarrow} \Big) \end{aligned} \tag{3.4}$$

3.1.1 Bogolioubov-de-Gennes transform

For diagrammatic expansion, it's convenient to work in the eigenbasis of the BCS and spin-ladder hamiltonian. This is achieved via a Bogoliubov-de-Gennes transform. The BdG transform for fermions is as follows,

$$\begin{aligned} \begin{pmatrix} c_{k\uparrow} \\ c^\dagger_{-k\downarrow} \end{pmatrix} = U_k \begin{pmatrix} f_{k\uparrow} \\ f^\dagger_{-k\downarrow} \end{pmatrix}, \quad U_k = \begin{pmatrix} u_k & v_k^* \\ -v_k & u_k \end{pmatrix}; \\ |u_k|^2 = \frac{1}{2}\left(1 + \frac{\xi_k}{E_k}\right), \quad |v_k|^2 = \frac{1}{2}\left(1 - \frac{\xi_k}{E_k}\right), \end{aligned} \tag{3.5}$$

where $E_k = (\xi_k^2 + |\Delta_k|^2)^{1/2}$ is the s-wave SC dispersion. We can choose u_k to be real and $\text{Arg}(v_k) = \text{Arg}(\Delta_k^*)$. while the BdG transform for bosons will be,

$$\begin{aligned} \vec{t}_k = \begin{pmatrix} W_k & Z^*_{-k} \\ Z_k & W^*_{-k} \end{pmatrix} \vec{\Gamma}_k, \quad & \vec{t}_k = \Big(t_{kx}, t_{ky}, t_{kz}, t^\dagger_{-kx}, t^\dagger_{-ky}, t^\dagger_{-kz} \Big)^T \\ & \vec{\Gamma}_k = \Big(\Gamma_{k1}, \Gamma_{k2}, \Gamma_{k3}, \Gamma^\dagger_{-k1}, \Gamma^\dagger_{-k2}, \Gamma^\dagger_{-k3} \Big)^T \end{aligned} \tag{3.6}$$

the analytical form of W_k, Z_k for the a hamiltonian like H_{SL} is quite complex. For our purposes, this form is good enough, as the coefficients can be computed numerically. From now on, we refer to f_k and Γ_k as fermionic and bosonic bogolons, respectively.

Manipulation of H_{int}

With this, we now rewrite everything in Eq.(3.4) in terms of bogolons. Starting with triplons operators, after normal ordering and some regrouping, the bosonic part takes the following form,

$$\begin{aligned} P_{k',-k} = \delta_{q+k'-k}(m'_{r,q} - n'_{r,q})\Gamma^\dagger_{qr} + \delta_{-q+k'-k}(n_{r,q} - m_{r,q})\Gamma_{qr} + \delta_{k'-k}\Xi_P \\ + \delta_{q'-q+k'-k}\Theta^P_{q,r} \cdot \Gamma^\dagger_{q'r}\Gamma_{qs} + (\cdots)\Gamma_{q'r}\Gamma_{qs} + (\cdots)\Gamma^\dagger_{q'r}\Gamma^\dagger_{qs} \\ Q_{k',-k} = \delta_{q+k'-k}(i w^*_{3s,q} - i z^*_{3s,q})\Gamma^\dagger_{qs} + \delta_{-q+k'-k}(i z_{3s,q} - i w_{3s,q})\Gamma_{qs} + \delta_{k'-k}\Xi_Q \\ + \delta_{q'-q+k'-k}\Theta^Q_{q,r} \cdot \Gamma^\dagger_{q'r}\Gamma_{qs} + (\cdots)\Gamma_{q'r}\Gamma_{qs} + (\cdots)\Gamma^\dagger_{q'r}\Gamma^\dagger_{qs} \end{aligned}$$

where,

$$\begin{aligned} m^{(\prime)}_{r,q} := w^{(*)}_{2r,q} + i w^{(*)}_{1r,q}; \qquad \Xi_P := i(z_{3r,q} n'_{r,q} - n_{r,q} z^*_{3r,q}); \\ n^{(\prime)}_{r,q} := z^{(*)}_{2r,q} + i z^{(*)}_{1r,q}; \qquad \Xi_Q := i(z_{2r,q} z^*_{1r,q} - z_{1r,q} z^*_{2r,q}); \end{aligned}$$

$$\begin{aligned} \Theta^P_{q,r} = i(w^*_{3r,q} m_{r,q} + n'_{r,q} z_{3r,q} - m'_{r,q} w_{3r,q} - z^*_{3r,q} n_{r,q}) \\ \Theta^Q_{q,r} = i(w^*_{2r,q} w_{1r,q} - w^*_{1r,q} w_{2r,q} + z^*_{1r,q} z_{2r,q} - z^*_{2r,q} z_{1r,q}). \end{aligned}$$

We do the same for the electron operators. Having everything in a symmetric form helps, so we write everything using spinors. We a priori define some coefficients,

$$g_{k',k} = u_{k'}u_k + v_{k'}v_k^*; \quad h_{k',k} = u_{k'}v_k^* - v_{k'}^*u_k,$$

and start with the re-writing of $\sigma^z_{\alpha\beta}c^\dagger_{k\alpha}c_{k\beta}$ term,

$$\begin{aligned}\sigma^z_{\alpha\beta}c^\dagger_{k'\alpha}c_{k\beta} &= \begin{pmatrix} c^\dagger_{k'\uparrow} & c_{-k'\downarrow}\end{pmatrix}\begin{pmatrix} c_{k\uparrow} \\ c^\dagger_{-k\downarrow}\end{pmatrix} - \delta_{k'k} \\ &= g_{k',k}\left(f^\dagger_{k'\uparrow}f_{k\uparrow} + f_{-k'\downarrow}f^\dagger_{-k\downarrow}\right) + \left(h_{k',k}f^\dagger_{k'\uparrow}f^\dagger_{-k\downarrow} + \text{h.c.}\right) - \delta_{k'k} \\ &= g_{k',k}\sigma^z_{\alpha\beta}f^\dagger_{k'\alpha}f_{k\beta} + \left(h_{k',k}f^\dagger_{k'\uparrow}f^\dagger_{-k\downarrow} + \text{h.c.}\right) - \delta_{k'k} + \delta_{k'k}g_{k'k},\end{aligned}$$

the $-\delta_{kk'}$, from permuting $-c^\dagger_\downarrow c_\downarrow$, would cancel the $g_{kk'}\delta_{kk'}$, from permuting $f_\downarrow f^\dagger_\downarrow$. Next, we do this for the spin-flipping terms. To make things symmetric, we take two copies of the spin flip term,

$$\frac{1}{2}\begin{pmatrix} c^\dagger_{k'\uparrow} & c_{-k'\downarrow}\end{pmatrix}\begin{pmatrix} 0 & 1 \\ -1 & 0\end{pmatrix}\begin{pmatrix} c^\dagger_{-k\uparrow} \\ c_{k\downarrow}\end{pmatrix} = \frac{1}{2}\begin{pmatrix} f^\dagger_{k'\uparrow} & f_{-k'\downarrow}\end{pmatrix}\begin{pmatrix} -h_{k',-k} & g_{k',-k} \\ g_{-k,k'} & -h^*_{k',-k}\end{pmatrix}\begin{pmatrix} f^\dagger_{-k\uparrow} \\ f_{k\downarrow}\end{pmatrix},$$

notice the off-diagonal terms are actually the same, related by the substitution $(k',k) \to (-k,-k')$. Therefore, the full expression for the spin-flip term is,

$$c^\dagger_{k'\uparrow}c_{k,\downarrow} = g_{k',-k}P_{k',-k}f^\dagger_{k'\uparrow}f_{k\downarrow} - \tfrac{1}{2}P_{k',-k}\left(h_{k',-k}f^\dagger_{k'\uparrow}f^\dagger_{-k\uparrow} + h^*_{k',-k}f_{-k'\downarrow}f_{k\downarrow}\right).$$

We rescale $g_{k',k}$ and $h_{k',k}$ by J_K, and put everything together to get the full interaction hamiltonian,

$$\begin{aligned}H_{\text{int}} &= g_{k',k}Q_{k',-k}\sigma^z_{\alpha\beta}f^\dagger_{k'\alpha}f_{k\beta} + \left(g_{k',-k}P_{k',-k}f^\dagger_{k'\uparrow}f_{k\downarrow} + \text{h.c.}\right) \\ &\quad + \left\{h_{k',k}Q_{k',-k}f^\dagger_{k'\uparrow}f^\dagger_{-k\downarrow} + P_{k',-k}\left(h_{k',-k}f^\dagger_{k'\uparrow}f^\dagger_{-k\uparrow} + h^*_{k',-k}f_{-k'\downarrow}f_{k\downarrow}\right) + \text{h.c.}\right\} \qquad (3.7) \\ g_{k',k} &= J_K(u_{k'}u_k + v_{k'}v_k^*); \quad h_{k',k} = J_K(u_{k'}v_k^* - v^*_{k'}u_k). \qquad (3.8)\end{aligned}$$

Now that we have a normal ordered expression, we can compute the corrections to superconductors due to H_{int}.

3.2 2^{nd} order corrections

To account for interaction, we will compute the corrections to the self energies using diagrammatic expansion. We will approximate the self energy with corrections up to second order i.e., one loop and one vertex diagrams. The justification is that since the triplon bands are gapped, diagrams with more than one boson line will be suppressed.

Also for the case of s-wave SC at zero temperature, some simplification occurs. The procedure is detailed in §A, here we only write the final result after simplification,

$$\Sigma^n_{\uparrow\uparrow}(k, ik_n) = g_{k,k}\Xi_Q - \sum_{k',r}\left(\frac{|g_{k',k}|^2 \cdot l^r_2(k-k')}{ik_n - E_{k'} - E^{\Gamma,r}_{k-k'}} + \frac{|h_{k,k'}|^2 \cdot l^r_1(-k-k')}{-ik_n - E_{k'} - E^{\Gamma,r}_{-k'-k}}\right) \qquad (3.9)$$

$$\Sigma^n_{\downarrow\downarrow}(k,ik_n) = g_{k,k}\Xi_Q - \sum_{k',r}\left(\frac{|g_{k',k}|^2\cdot l_3^r(k-k')}{ik_n - E_{k'} - E^{\Gamma,r}_{k-k'}} + \frac{|h_{k,k'}|^2\cdot l_1^r(-k-k')}{-ik_n - E_{k'} - E^{\Gamma,r}_{-k'-k}}\right) \tag{3.10}$$

$$\Sigma^n_{\uparrow\downarrow}(k,ik_n) = g_{k,k}\Xi_P - \sum_{k',r} g^2_{k',k}\frac{l_4^r(k-k') - l_5^r(k-k')}{ik_n - E_{k'} - E^{\Gamma,r}_{k-k'}} \tag{3.11}$$

$$\Sigma^a_{\uparrow\uparrow}(k,ik_n) = -\sum_{k',r} g_{k,k'}h_{k,k'}\left(\frac{l_5^{r*}(k-k')}{ik_n - E_{k'} - E^{\Gamma,r}_{k-k'}} - \frac{l_5^{r*}(-k-k')}{-ik_n - E_{k'} - E^{\Gamma,r}_{-k-k'}}\right) \tag{3.12}$$

$$\Sigma^a_{\downarrow\downarrow}(k,ik_n) = -\sum_{k',r} g_{k,k'}h_{k,k'}\left(\frac{l_4^{r}(k-k')}{ik_n - E_{k'} - E^{\Gamma,r}_{k-k'}} - \frac{l_4^{r}(-k-k')}{-ik_n - E_{k'} - E^{\Gamma,r}_{-k-k'}}\right) \tag{3.13}$$

$$\Sigma^a_{\downarrow\uparrow}(k,ik_n) = -\sum_{k',r} g_{k',k}h_{k,k'}\left(\frac{l_1^{r}(-k-k')}{-ik_n - E_{k'} - E^{\Gamma,r}_{-k-k'}} + \frac{l_1^{r}(k-k')}{ik_n - E_{k'} - E^{\Gamma,r}_{k-k'}}\right) \tag{3.14}$$

where,

$$l_1^r(q) = |w_{3r,q} - z_{3r,q}|^2,$$
$$l_2^r(q) = 2\cdot l_1^r(q) + |n_{r,q} - m_{r,q}|^2, \quad l_3^r(q) = 2\cdot l_1^r(q) + |m'_{r,q} - n'_{r,q}|^2,$$
$$l_4^r(q) = (m'_{r,q} - n'_{r,q})(iz_{3r,q} - iw_{3r,q}), \quad l_5^r(q) = (n_{r,q} - m_{r,q})(iz_{3r,q} - iw_{3r,q})^*,$$

E_k and $E_k^{\Gamma,r}$ are the SC and triplon band energies, respectively.

It is worth mentioning that self energies must satisfy certain properties regardless of the details of the interaction. These are really properties of the propagators from which self energies are derived,

$$\Sigma^n_{\alpha\beta}(k,\tau) \sim \left\langle f_{k\alpha}(\tau)\cdots f^\dagger_{k\beta}(0)\right\rangle = \left\langle f_{k\beta}(0)\cdots f^\dagger_{k\alpha}(-\tau)\right\rangle^* \sim \Sigma^n_{\beta\alpha}(k,\tau)^*$$
$$\Sigma^a_{\alpha\beta}(k,\tau) \sim \left\langle f^\dagger_{-k\alpha}(\tau)\cdots f^\dagger_{k\beta}(0)\right\rangle = -\left\langle f^\dagger_{k\beta}(0)\cdots f^\dagger_{-k\alpha}(\tau)\right\rangle \sim -\Sigma^a_{\beta\alpha}(-k,-\tau).$$

Therefore,

$$\Sigma^n_{\alpha\beta}(k,ik_n) = \Sigma^n_{\beta\alpha}(k,-ik_n)^*, \quad \Sigma^a_{\alpha\beta}(k,ik_n) = -\Sigma^a_{\beta\alpha}(-k,-ik_n) \tag{3.15}$$

The Green's function

Due to the pair creation and annihilation term in Eq.(3.7), we expect the interaction to induce anomalous pairings of both singlet and triplet type. Moreover, anomalous triplet order parameter $\langle c^\dagger_\alpha c^\dagger_\alpha\rangle$ is vital for diagnosing topological superconductivity. Thus, to capture these contributions, we pick the spinor to be,

$$\psi_k(\tau) := (c_{k\uparrow}(\tau), c_{k\downarrow}(\tau), c^\dagger_{-k\uparrow}(\tau), c^\dagger_{-k\downarrow}(\tau))^T$$

the corresponding Green's function matrix would then be,

$$\hat{G}(k,\tau) = \left\langle T_\tau \psi(\tau)\psi^\dagger(0)\right\rangle = \begin{pmatrix}\mathbf{G}(k,\tau) & \mathbf{F}^\dagger(k,\tau)\\ \mathbf{F}(k,\tau) & -\mathbf{G}^T(-k,-\tau)\end{pmatrix}, \tag{3.16}$$
$$[\mathbf{G}(k,\tau)]_{\alpha\beta} = \left\langle c_{k\alpha}(\tau)c^\dagger_{k\beta}(0)\right\rangle, \quad [\mathbf{F}(k,\tau)]_{\alpha\beta} = \left\langle c^\dagger_{-k\alpha}(\tau)c^\dagger_{k\beta}(0)\right\rangle.$$

To proceed, we need to convert from electronic basis to bogolonic basis. For this purpose, we define the following,

$$\phi(\tau) := (f_{k\uparrow}(\tau), f_{k\downarrow}(\tau), f^{\dagger}_{-k\uparrow}(\tau), f^{\dagger}_{-k\downarrow}(\tau))^T, \quad \hat{G}_f(k,\tau) = \left\langle T_\tau \phi(\tau)\phi^\dagger(0) \right\rangle, \quad (3.17)$$

next we define the basis change via $\psi_k(\tau) = T_k \phi_k(\tau)$ where,

$$T = \begin{pmatrix} u_k & & & v^*_k \\ & u_{-k} & -v^*_{-k} & \\ & v_{-k} & u_{-k} & \\ -v_k & & & u_k \end{pmatrix}.$$

Thus, Eq.(3.16) and Eq.(3.17) are related by, $\hat{G}(k,ik_n) = T_k \hat{G}_f(k,ik_n) T_k^\dagger$. Finally, we switch to frequency space, then via dyson series expansion, we make use of the self energy expressions we just derived,

$$\hat{G}(k,ik_n) = T_k \hat{G}_f(k,ik_n) T_k^\dagger \quad (3.18)$$

$$\hat{G}_f(k,ik_n) = \begin{pmatrix} ik_n - E_k - \hat{\Sigma}^n(k,ik_n) & -\hat{\Sigma}^a(k,-ik_n)^\dagger \\ -\hat{\Sigma}^a(k,ik_n) & ik_n + E_k + \hat{\Sigma}^n(-k,-ik_n)^T \end{pmatrix}^{-1} \quad (3.19)$$

$$\hat{\Sigma}^n(k,ik_n) = \begin{pmatrix} \Sigma^n_{\uparrow\uparrow}(k,ik_n) & \Sigma^n_{\uparrow\downarrow}(k,ik_n) \\ \Sigma^n_{\downarrow\uparrow}(k,ik_n) & \Sigma^n_{\downarrow\downarrow}(k,ik_n) \end{pmatrix}, \quad \hat{\Sigma}^a(k,ik_n) = \begin{pmatrix} \Sigma^a_{\uparrow\uparrow}(k,ik_n) & \Sigma^a_{\uparrow\downarrow}(k,ik_n) \\ \Sigma^a_{\downarrow\uparrow}(k,ik_n) & \Sigma^a_{\downarrow\downarrow}(k,ik_n) \end{pmatrix}$$

3.3 Resultant topological class

One may expect that the topology of an interacting system is captured by the effective Green's function. However, Wang and Yan showed that this turns out not to be the case [28]. They also propose a fix, called the topological hamiltonian, defined as,

$$h_{\text{top}}(k) = \hat{G}^{-1}(k,0) = \hat{G}_0^{-1}(k,0) - \Sigma(k,0) = h_0(k) - \Sigma(k,0)$$

where, h_0 and $\hat{G}_0$ are the bare free hamiltonian and Green's function, respectively. They showed that h_{top} shares the same topological invariant as the interacting system, and thus accurately captures its topology.

For our case we can make use of Eq.(3.18,3.19) and get,

$$h_{\text{top}}(k) = \hat{G}^{-1}(k,0) = T_k \begin{pmatrix} -E_k - \hat{\Sigma}^n(k,0) & -\hat{\Sigma}^a(k,0)^\dagger \\ -\hat{\Sigma}^a(k,0) & E_k + \hat{\Sigma}^n(-k,0)^T \end{pmatrix} T_k^\dagger. \quad (3.20)$$

If we can identify the symmetries of $h_{\text{top}}(k)$, then we can use the AZ classification to get the topological class of our interfaced SC. Although it's not possible to write a general analytical formula for the self energies, but we can still simplify for certain parameter regimes.

Setting h_y to zero. In this limit, the triplon hamiltonian matrices from Eq.(2.2) and Eq.(2.5), both reduce to the form,

$$h(k) = \begin{pmatrix} h_1(k) & h_2(k) \\ h_2^\dagger(k) & h_1(k) \end{pmatrix}; \quad \begin{matrix} h_1(k) = (J + J'\cos(k))\mathbb{I} + \mathbf{d}\cdot\mathbf{Z}; \\ h_2(k) = -J' e^{-ik}\mathbb{I} - \mathbf{d}\cdot\mathbf{Z} \end{matrix}, \quad (3.21)$$

where, $d = (\Gamma\cos(k), -D\sin(k), 0)$ and $\mathbf{Z}$ can be either σ or $\mathbf{L}$ vector of matrices from §2.1 or §2.2, respectively. Notice, the hamiltonian follows the relation,

$$h(-k) = h(k)^*,$$

and so should the BdG coefficients i.e., $W_{-k}(Z_{-k}) = W_k^*(Z_k^*)$, therefore,

$$m'_k - n'_k = m_{-k} - n_{-k}, \tag{3.22}$$

Additionally, in this limit the BdG coefficients can be written analytically, since h_1 and h_2 now commute, details are in §B. Using the exact form of W_k and Z_k, we get,

$$|m_k - n_k| = |m_{-k} - n_{-k}|, \tag{3.23}$$

3.3.1 Symmetries of h_{top}

To simplify the search we will first derive some relations. First, note that the self energies in Eq.(3.20) are evaluated at $ik_n = 0$. In this limit,

- $\Sigma^n_{\uparrow\uparrow}(k,0)$ is purely real, and $\Sigma^a_{\uparrow\uparrow}(k,0)$ is odd, using Eq.(3.15).
- $\Sigma^a_{\downarrow\uparrow}(k,0)$ is purely real and even w.r.t k, via Eq.(3.14)

Bringing the relations we get for $h_y = 0$, leads to further simplification,

- $\Sigma^n_{\uparrow\uparrow}(k,0) = \Sigma^n_{\downarrow\downarrow}(k,0)$ and $\Sigma^a_{\uparrow\uparrow}(k,0) = -\Sigma^a_{\downarrow\downarrow}(k,0)^*$, via Eq.(3.22) .
- $\Sigma^n_{\uparrow\uparrow}(k,0)$ is even and $\Sigma^n_{\uparrow\downarrow}(k,0)$ is odd w.r.t k, via Eq.(3.23).

Next, we break down the h_{top} into a sum of Gamma matrices. Certain terms get eliminated using the above relations. Starting with $G_f(k,0)$, recall Eq.(3.19),

$$\begin{aligned} G_f(k,0)^{-1} = &(E_k + \Sigma^n_{\uparrow\uparrow}(k)) \cdot \sigma_z \otimes \mathbb{I} + \Sigma^a_{\downarrow\uparrow}(k) \cdot \sigma_y \otimes \sigma_y \\ &+ \text{Re}[\Sigma^n_{\uparrow\downarrow}(k)] \cdot \mathbb{I} \otimes \sigma_x + \text{Im}[\Sigma^n_{\uparrow\downarrow}(k)] \cdot \sigma_z \otimes \sigma_y. \\ &+ \text{Re}[\Sigma^a_{\uparrow\uparrow}(k)] \cdot \sigma_x \otimes \sigma_z + \text{Im}[\Sigma^a_{\uparrow\uparrow}(k)] \cdot \sigma_y \otimes \mathbb{I} \end{aligned} \tag{3.24}$$

The first line contains terms that are even w.r.t k, while the rest contains odd terms.

In momentum basis, the symmetry operator relations will look slightly different than the ones in Eq.(1.4). For our case,

$$\begin{aligned} &\text{TRS}: \quad h(k) = T h(-k)^T T^{-1}, \quad T^T = -T \\ &\text{PHS}: \quad h(k) = -P h(-k)^T P^{-1}, \quad P^T = \pm P \end{aligned} \ . \tag{3.25}$$

For now, we only focus on symmetries of G_f^{-1}. Based on Eq.(3.25) and Eq.(3.24), T must anti-commute with $\mathbb{I} \otimes \sigma_x$, $\sigma_x \otimes \sigma_z$, and commute with other matrices of Eq.(3.24). Whereas for P, the condition is reversed. One possible solution for each of them is,

$$P = \sigma_x \otimes \mathbb{I}, \quad T = \mathbb{I} \otimes \sigma_y. \tag{3.26}$$

Luckily these also commute with T_k, since $T_k = u_k \cdot \mathbb{I} + i v_k \cdot \sigma_x \otimes \sigma_y$. Thus, these are symmetries of the full h_{top}, putting it in DIII class of AZ classification, see Table.1.1. Therefore, our system can possibly show a non-trivial $\mathbb{Z}_2$ invariant.

3.3.2 Calculation of $\mathbb{Z}_2$ invariant for DIII class

We follow the method detailed in [29]. A benefit of this approach is that it is gauge invariant or basis independent. First, we select a discrete set of points from the Brillouin zone, say $k_a = \pi a/N$. Let $\{|u_\alpha(k)\rangle\}_\alpha$ be the eigenfunctions of occupied bands at point k. Now we define the following quantities, first the Kato propagator,

$$\mathscr{U}_K = \prod_{i=0}^{N} P(k_i)\,, \quad P(k) = \sum_{\alpha\in\text{occ}} |u_\alpha(k)\rangle\langle u_\alpha(k)| \tag{3.27}$$

the product should be ordered, as in i increases from going right to left. Next, let $\mathscr{T}$ be the time reversal operator,

$$[\Theta(k)]_{\alpha\beta} = \langle u_\alpha(k)|\mathscr{T}|u_\beta(k)\rangle.$$

Note that $\mathscr{T}$ is different from the unitary T in Eq.(3.26), the two are related by $\mathscr{T} = TK$ where K is the complex conjugation operator. Lastly, we define,

$$[U_K]_{\alpha\beta} = \langle u_\alpha(\pi)|\mathscr{U}_K|u_\beta(0)\rangle.$$

The $\mathbb{Z}_2$ invariant ν, is then given by,

$$(-1)^\nu = \det(U_K)\frac{\text{Pf}(\Theta(0))}{\text{Pf}(\Theta(\pi))} \tag{3.28}$$

where, Pf stands for Pfaffian of the matrix.

Lastly, if the system has inversion symmtery i.e., there exists an operator P_I such that $P_I h(-k)P_I = h(k)$, then the formula reduces to simply,

$$(-1)^\nu = \prod_{\alpha\in\text{occ}} \xi_\alpha(0)\xi_\alpha(\pi), \tag{3.29}$$

where, $\xi_\alpha(k)$ is the eigenvalue of $|u_\alpha(k)\rangle$ w.r.t the inversion operator P_I. Luckily, our system is inversion symmetric, the operator is,

$$P_I = \sigma_z \otimes \sigma_z$$

Chapter 4

Results

All important quantities from the previous chapter, as well as the ones in this chapter, require the computation of self energies. As mentioned in the previous chapter, a complete analytical expression is not possible. Thus, we use numerics to approximate them.

In this chapter, we report the resultant bands of topological hamiltonian and order parameters. To support these, we also show the calculated spectral function of the superconducting subsystem. Lastly, we report if there is a non-trivial $\mathbb{Z}_2$ invariant.

4.1 Effects of interaction

4.1.1 Spectral function

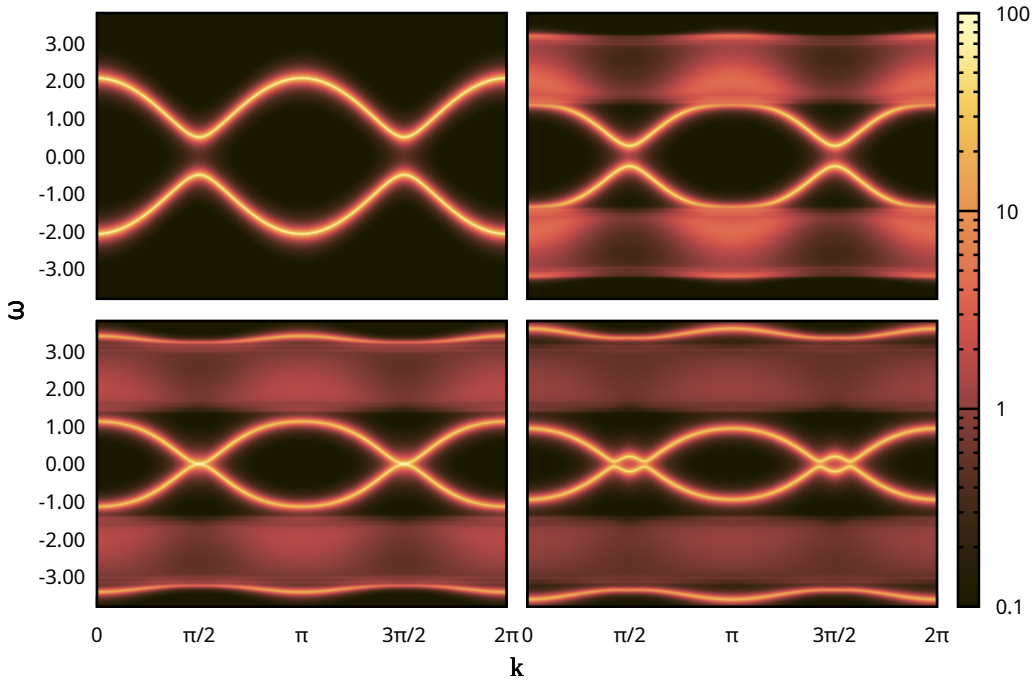

Figure 4.1: Spectral function. Evaluated at (a) $J_K = 0.0$, (b) $J_K = 1.0J$, (c) $J_K = 1.6J$, (d) $J_K = 2.4J$

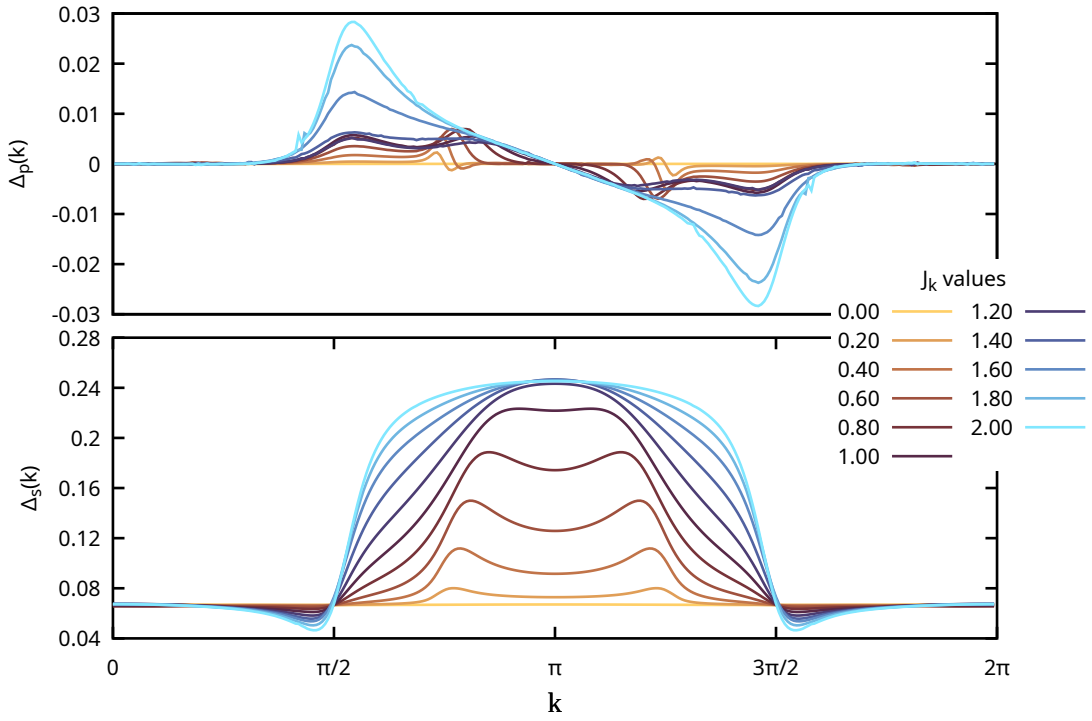

Figure 4.2: Anomalous pairing order parameters.

The spectral function can be computed from Eq.(3.18, 3.19). The expression for the spectral function is,

$$A(k,\omega) = -2 \cdot \mathrm{Im}\left[\mathrm{Tr}(\hat{G}(k,\omega))\right].$$

to get the Green's function in terms of real frequency use analytic continuation, $ik_n \to \omega + i\eta$ where η is infinitesimal positive number.

Fig.4.1 shows the variation in spectral function as the Kondo coupling is increased. This is a strong indication that the bands of the interacting superconductor do cross and reopen at around $J_K/J \sim 1.6$. All graphs from this point onwards are evaluated at parameter values $K = 0.01J, D = \Gamma = 0.1J, h_y = 0$ useless stated otherwise.

4.1.2 Order parameters

The order parameters we are interested in are the anomalous triplet and singlet pairings. They can be calculated as follows,

$$\Delta_k^p = \left\langle c^\dagger_{-k\uparrow}(0) c^\dagger_{k\uparrow}(0) \right\rangle = [\hat{G}(k,0)]_{02} = \int_{-\infty}^{\infty} d\omega\, [\hat{G}(k,\omega)]_{02}$$

$$\Delta_k^s = \left\langle c^\dagger_{-k\downarrow}(0) c^\dagger_{k\uparrow}(0) \right\rangle = [\hat{G}(k,0)]_{03} = \int_{-\infty}^{\infty} d\omega\, [\hat{G}(k,\omega)]_{03}$$

Fig.4.2 shows the final result, and it clearly shows that interactions do induce a p-wave like pairing.

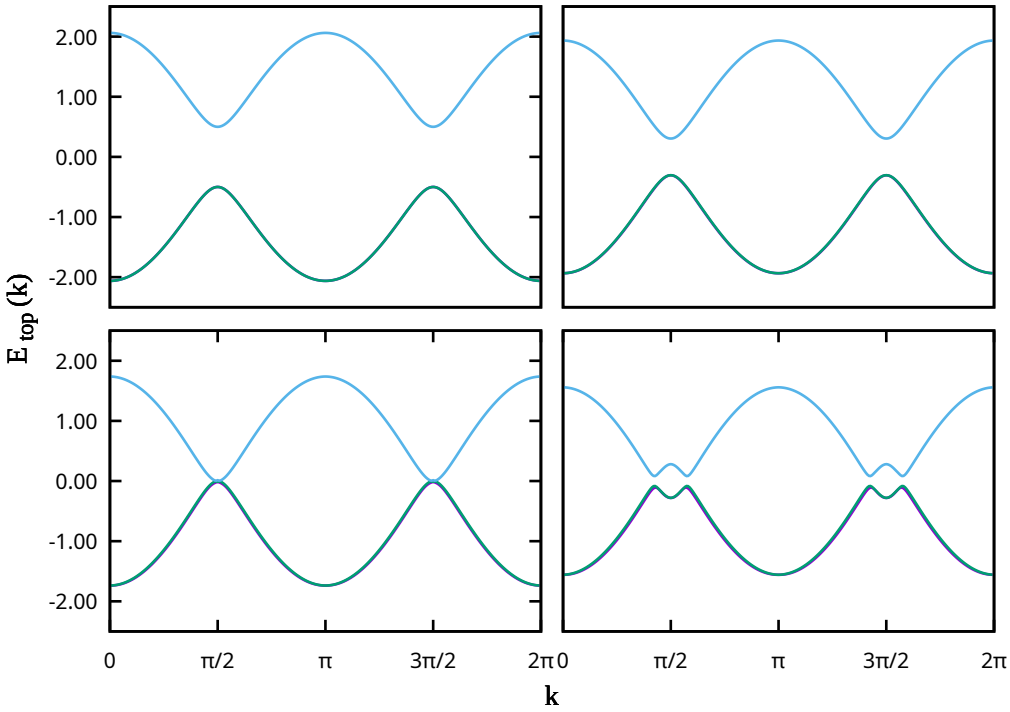

Figure 4.3: Dispersion bands of $h_{\text{top}}(k)$. Evaluated at same J_K values as spectral function i.e., (a) $J_K = 0.0$, (b) $J_K = 1.0J$, (c) $J_K = 1.6J$, (d) $J_K = 2.4J$

4.2 Signs of non-trivial topological phase

The dispersion of h_{top} and spectral function are in good agreement, they show band crossing at around the same Kondo strength, see Fig.4.3. So, there can be a topological phase transition around the point $J_K = 1.6J$.

To confirm the existence of a non-trivial topological phase, we compute the $\mathbb{Z}_2$ for different values of J_K, using the procedure detailed in the previous chapter. The final result is shown in Fig.4.4.

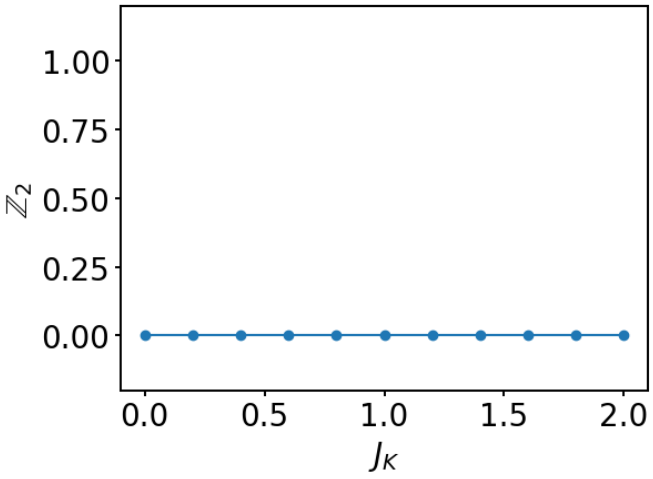

Figure 4.4: The $\mathbb{Z}_2$ invariant.

4.3 Summary and Outlook

In this work, we showed that interfacing an s-wave SC with a spin-ladder lattice, gives rise to a triplet pairing, even though the two subsystems are time-reversal symmetric. Moreover, the spin ladder being a paramagnet, lacks magnetic order. Hence, this effect arises solely from the dynamics of the triplons, and cannot be captured by a mean-field description. Our work broadens the domain of unconventional SCs in SC-magnet heterostructures. Being induced from a Kondo interaction also makes it experimentally accessible.

Although there is a band gap closing and reopening, we don't find any topological phase with a non-trivial $\mathbb{Z}_2$ invariant. There are still possibilities that the system can support a topological phase. One place to explore would be the non-zero magnetic field regime, where the time reversal symmetry is broken. The system would now be in the D class, which does support a $\mathbb{Z}_2$ invariant, the calculation is slightly non-trivial. In fact, there is still a remaining possibility in the zero magnetic field case, which is the existence of a $\mathbb{Z}_8$ invariant [24].

Lastly, we also intend to apply this approach to 2D systems, in particular the s-wave SC interfaced with the Kitaev-Heisenberg (KH) lattice. The KH spin lattice, is known to host topological phases [30]. Unlike the spin-ladder, it is gapless and ferromagnetic. We hope it can lead to stronger and richer dynamics than the ones we studied here.

Bibliography

[1] A Yu Kitaev. Unpaired majorana fermions in quantum wires. *Physics-Uspekhi*, 44(10S):131, oct 2001.

[2] Michael Freedman, Alexei Kitaev, Michael Larsen, and Zhenghan Wang. Topological quantum computation. *Bulletin of the American Mathematical Society*, 40(1):31–38, 2003.

[3] Michael H Freedman. P/np, and the quantum field computer. *Proceedings of the National Academy of Sciences*, 95(1):98–101, 1998.

[4] A.Yu. Kitaev. Fault-tolerant quantum computation by anyons. *Annals of Physics*, 303(1):2–30, 2003.

[5] Chetan Nayak, Steven H. Simon, Ady Stern, Michael Freedman, and Sankar Das Sarma. Non-abelian anyons and topological quantum computation. *Rev. Mod. Phys.*, 80:1083–1159, Sep 2008.

[6] J Q You, Z D Wang, Wenxian Zhang, and Franco Nori. Encoding a qubit with majorana modes in superconducting circuits. *Scientific Reports*, 4(1):5535, jul 2014.

[7] John McGreevy and Brian Swingle. Non-abelian statistics versus the witten anomaly. *Phys. Rev. D*, 84:065019, Sep 2011.

[8] Richard Hess, Henry F. Legg, Daniel Loss, and Jelena Klinovaja. Trivial andreev band mimicking topological bulk gap reopening in the nonlocal conductance of long rashba nanowires. *Phys. Rev. Lett.*, 130:207001, May 2023.

[9] Haining Pan, Chun-Xiao Liu, Michael Wimmer, and Sankar Das Sarma. Quantized and unquantized zero-bias tunneling conductance peaks in majorana nanowires: Conductance below and above $2e^2/h$. *Phys. Rev. B*, 103:214502, Jun 2021.

[10] Igor J. Califrer, Poliana H. Penteado, J. Carlos Egues, and Wei Chen. Proximity-induced zero-energy states indistinguishable from topological edge states. *Phys. Rev. B*, 107:045401, Jan 2023.

[11] Pasquale Marra and Angela Nigro. Majorana/andreev crossover and the fate of the topological phase transition in inhomogeneous nanowires. *Journal of Physics: Condensed Matter*, 34(12):124001, jan 2022.

[12] Wei Chen and Andreas P. Schnyder. Majorana edge states in superconductor-noncollinear magnet interfaces. *Phys. Rev. B*, 92:214502, Dec 2015.

[13] T.-P. Choy, J. M. Edge, A. R. Akhmerov, and C. W. J. Beenakker. Majorana fermions emerging from magnetic nanoparticles on a superconductor without spin-orbit coupling. *Phys. Rev. B*, 84:195442, Nov 2011.

[14] Maxime Garnier, Andrej Mesaros, and Pascal Simon. Topological superconductivity with deformable magnetic skyrmions. *Communications Physics*, 2(1):"126", oct 2019.

[15] Sho Nakosai, Yukio Tanaka, and Naoto Nagaosa. Two-dimensional p-wave superconducting states with magnetic moments on a conventional s-wave superconductor. *Phys. Rev. B*, 88:180503, Nov 2013.

[16] K. v. Klitzing, G. Dorda, and M. Pepper. New method for high-accuracy determination of the fine-structure constant based on quantized hall resistance. *Phys. Rev. Lett.*, 45:494–497, Aug 1980.

[17] B Jeckelmann and B Jeanneret. The quantum hall effect as an electrical resistance standard. *Reports on Progress in Physics*, 64(12):1603, nov 2001.

[18] M E Suddards, A Baumgartner, M Henini, and C J Mellor. Scanning capacitance imaging of compressible and incompressible quantum hall effect edge strips. *New Journal of Physics*, 14(8):083015, aug 2012.

[19] Qian Niu, D. J. Thouless, and Yong-Shi Wu. Quantized hall conductance as a topological invariant. *Phys. Rev. B*, 31:3372–3377, Mar 1985.

[20] Alexander Altland and Martin R. Zirnbauer. Nonstandard symmetry classes in mesoscopic normal-superconducting hybrid structures. *Phys. Rev. B*, 55:1142–1161, Jan 1997.

[21] Andreas P. Schnyder, Shinsei Ryu, Akira Furusaki, and Andreas W. W. Ludwig. Classification of topological insulators and superconductors in three spatial dimensions. *Phys. Rev. B*, 78:195125, Nov 2008.

[22] Shinsei Ryu, Andreas P Schnyder, Akira Furusaki, and Andreas W W Ludwig. Topological insulators and superconductors: tenfold way and dimensional hierarchy. *New Journal of Physics*, 12(6):065010, jun 2010.

[23] Anton Kapustin, Ryan Thorngren, Alex Turzillo, and Zitao Wang. Fermionic symmetry protected topological phases and cobordisms. *Journal of High Energy Physics*, 2015(12):1–21, dec 2015.

[24] Lukasz Fidkowski and Alexei Kitaev. Topological phases of fermions in one dimension. *Phys. Rev. B*, 83:075103, Feb 2011.

[25] A. Collins, C. J. Hamer, and Zheng Weihong. Modified triplet-wave expansion method applied to the alternating heisenberg chain. *Phys. Rev. B*, 74:144414, Oct 2006.

[26] Darshan G. Joshi, Kris Coester, Kai P. Schmidt, and Matthias Vojta. Nonlinear bond-operator theory and $1/d$ expansion for coupled-dimer magnets. i. paramagnetic phase. *Phys. Rev. B*, 91:094404, Mar 2015.

[27] Darshan G. Joshi and Andreas P. Schnyder. Topological quantum paramagnet in a quantum spin ladder. *Phys. Rev. B*, 96:220405, Dec 2017.

[28] Zhong Wang and Binghai Yan. Topological hamiltonian as an exact tool for topological invariants. *Journal of Physics: Condensed Matter*, 25(15):155601, mar 2013.

[29] Jan Carl Budich and Eddy Ardonne. Topological invariant for generic one-dimensional time-reversal-symmetric superconductors in class diii. *Phys. Rev. B*, 88:134523, Oct 2013.

[30] Darshan G. Joshi. Topological excitations in the ferromagnetic kitaev-heisenberg model. *Phys. Rev. B*, 98:060405, Aug 2018.

Appendix A

Feynman-diagrammatic corrections to self energies

Table.A.1 shows the propagators we need to compute to get the self energies.

First consider the loop diagrams, any non-vanishing bracket must have 3 $ff^\dagger$ pairs with matching spins. In table.A.2 we group interaction terms based on whether they conserve spin or particle number. With this, we can deduce which combinations of H_I's won't vanish. Single vertex diagrams are straightforward, as there is only one possibility in each case.

Any bracket with terms like $f^\dagger_\alpha f^\dagger_\alpha$ automatically vanishes due to permutations from Wick's theorem. Next, we include the bosonic terms. Single loop shall only have a $\Gamma\Gamma^\dagger$ pair, hence only keep linear orders from $P_{kk'}$ and $Q_{kk'}$. The allowed terms for one vertex diagrams are a lot simpler, and we will add them directly to the final expression.

We introduce the following notation. For convenience, we put placeholders for external lines while writing self energy diagrams,

1. Vertex with incoming spin up (down) fermion: ◠ (◡);
   Vertex with outgoing spin up (down) fermion: ⌓ (⌔)
2. $G^f_{\uparrow\uparrow}(k, ik_n) \equiv$ ⟶●⟶; $G^f_{\downarrow\downarrow}(k, ik_n) \equiv$ ⟶●⟶; $G^\Gamma(k, ik_n) \equiv$ - - -►- - -
3. - - -◄- - - + - - -►- - - = - - - - - - - -

Self energy type	One vertex diag.	One loop diag.
Normal, Σ^n	$\left\langle T_\tau f_{k\alpha}(\tau) H_I(\tau_1) f^\dagger_{k\beta}(0) \right\rangle$	$\left\langle T_\tau f_{k\alpha}(\tau) H_I(\tau_1) H_I(\tau_2) f^\dagger_{k\beta}(0) \right\rangle$
Anomalous, Σ^a	$\left\langle T_\tau f^\dagger_{-k\alpha}(\tau) H_I(\tau_1) f^\dagger_{k\beta}(0) \right\rangle$	$\left\langle T_\tau f^\dagger_{-k\alpha}(\tau) H_I(\tau_1) H_I(\tau_2) f^\dagger_{k\beta}(0) \right\rangle$

Table A.1: Propogators for a given self energy. H_I is placeholder for any term in H_{int}

(a) Different kinds of terms

Same spin	Preserves # particle	Interaction terms
Yes	Yes	(1) $g_{k',k} f^\dagger_{k'\alpha} f_{k,\alpha}$
No	Yes	(2) $g_{k',-k} f^\dagger_{k'\uparrow} f_{k\downarrow}$ (3) $g^*_{k',-k} f^\dagger_{k\downarrow} f_{k'\uparrow}$
No	No	(4) $h_{k',k} f^\dagger_{k'\uparrow} f^\dagger_{-k\downarrow}$ (5) $h^*_{k',k} f_{-k\downarrow} f_{k'\uparrow}$

(b) Allowed terms in H_Is

Condition	$\langle f_{k\alpha} \cdots f^\dagger_{k\beta} \rangle$	$\langle f^\dagger_{-k\alpha} \cdots f^\dagger_{k\beta} \rangle$
$\alpha = \beta$	(1,1), (2,3), (4,5)	(2,5)
$\alpha \neq \beta$	(1,2/3)	(1,5)

Table A.2: Allowed vertices in single loop diagrams. The trick is to match the type of interaction with the type of external operators. For example, in $\langle f_{k\uparrow} \cdots f^\dagger_{k\downarrow} \rangle$ the external operators save particle number but not spin, thus a pair of interactions, where one is picked from row 1, and 2 should work.

Finally, we apply Wick's theorem and get the self energy expressions,

$\Sigma^n_{\uparrow\uparrow} = 2 \cdot$ 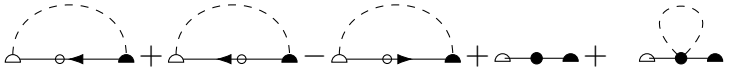 (A.1)

$\Sigma^n_{\uparrow\downarrow} =$ 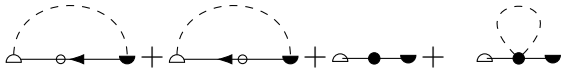 (A.2)

$\Sigma^a_{\uparrow\uparrow} =$ 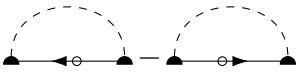 (A.3)

$\Sigma^a_{\downarrow\uparrow} =$  (A.4)

All that's left is to put appropriate interaction vertices in Eq.(A.1-A.4). The resultant expressions are,

$$\begin{aligned}\Sigma^n_{\uparrow\uparrow}(k) = \frac{-1}{\beta}\sum_{k',p}\Big(&2G^f_{\uparrow\uparrow}(k')G^\Gamma_r(q)\cdot|g_{k',k}|^2|w_{3r,q}-z_{3r,q}|^2\cdot\left(\delta_{q+k'-k}+\delta_{q+k-k'}\right)\\ &+G^f_{\downarrow\downarrow}(k')G^\Gamma_r(q)\cdot|g_{k,-k'}|^2\left(|m'_{r,q}-n'_{r,q}|^2\delta_{q+k-k'}+|n_{r,q}-m_{r,q}|^2\delta_{q+k'-k}\right)\\ &-G^f_{\downarrow\downarrow}(k')G^\Gamma_r(q)\cdot|h_{k,-k'}|^2|w_{3r,q}-z_{3r,q}|^2\cdot\left(\delta_{q+k+k'}+\delta_{q-k-k'}\right)\Big)\\ &+g_{k,k}(\Xi_Q+\Theta^Q_{q,r}\cdot G^\Gamma_r(q))\end{aligned} \tag{A.5}$$

$$\begin{aligned}\Sigma^n_{\uparrow\downarrow}(k) = \frac{-1}{\beta}\sum_{k',p}\Big(&G^f_{\uparrow\uparrow}(k')G^\Gamma_r(q)\cdot g_{k',-k}g_{k,k'}\big((m'_{r,q}-n'_{r,q})(iz_{3r,q}-iw_{3r,q})\cdot\delta_{q+k'-k}\\ &+(iz_{3r,q}-iw_{3r,q})^*(n_{r,q}-m_{r,q})\cdot\delta_{q+k-k'}\big)\\ &-G^f_{\downarrow\downarrow}(k')G^\Gamma_r(q)\cdot g_{k',k}g_{k,-k'}\big((m'_{r,q}-n'_{r,q})(iz_{3r,q}-iw_{3r,q})\cdot\delta_{q+k-k'}\\ &+(iz_{3r,q}-iw_{3r,q})^*(n_{r,q}-m_{r,q})\cdot\delta_{q+k'-k}\big)\Big)\\ &+g_{k,k}(\Xi_P+\Theta^P_{q,r}\cdot G^\Gamma_r(q))\end{aligned} \tag{A.6}$$

$$\begin{aligned}\Sigma^a_{\uparrow\uparrow}(k) = \tfrac{-1}{\beta}\sum_{k',p}\Big(&G^f_{\downarrow\downarrow}(k')G^\Gamma_r(q)\cdot g^*_{k,-k'}h^*_{-k,-k'}\big((m'_{r,q}-n'_{r,q})^*(iz_{3r,q}-iw_{3r,q})^*\cdot\delta_{q+k-k'}\\&+(iz_{3r,q}-iw_{3r,q})(n_{r,q}-m_{r,q})^*\cdot\delta_{q+k'-k}\big)\\&-G^f_{\downarrow\downarrow}(k')G^\Gamma_r(q)\cdot h^*_{k,-k'}g^*_{-k,-k'}\big((m'_{r,q}-n'_{r,q})^*(iz_{3r,q}-iw_{3r,q})^*\cdot\delta_{q-k-k'}\\&+(iz_{3r,q}-iw_{3r,q})(n_{r,q}-m_{r,q})^*\cdot\delta_{q+k'+k}\big)\Big)\end{aligned} \tag{A.7}$$

$$\begin{aligned}\Sigma^a_{\downarrow\uparrow}(k) = \tfrac{-1}{\beta}\sum_{k',p}\Big(&G^f_{\downarrow\downarrow}(k')G^\Gamma_r(q)\cdot g_{k',-k}h^*_{k,-k'}|w_{3r,q}-z_{3r,q}|^2\left(\delta_{q+k+k'}+\delta_{q-k-k'}\right)\\&-G^f_{\uparrow\uparrow}(k')G^\Gamma_r(q)\cdot g_{k',k}h^*_{k',k}|w_{3r,q}-z_{3r,q}|^2\left(\delta_{q+k'-k}+\delta_{q-k'+k}\right)\Big)\\&-h^*_{k,k}(\Xi_Q+\Theta_Q)\end{aligned} \tag{A.8}$$

where,

$$\begin{aligned}\Theta_P &= i(w^*_{3r,q}m_{r,q}+n'_{r,q}z_{3r,q}-m'_{r,q}w_{3r,q}-z^*_{3r,q}n_{r,q})\cdot G^\Gamma_r(q)\\ \Theta_Q &= i(w^*_{2r,q}w_{1r,q}-w^*_{1r,q}w_{2r,q}+z^*_{1r,q}z_{2r,q}-z^*_{2r,q}z_{1r,q})\cdot G^\Gamma_r(q)\end{aligned}$$

Flipping all spins in previous diagrams get us the remaining ones. This amounts to replacing $g_{k,-k'}P_{k,-k'}$ with its h.c and switch k and k'. Likewise in $h^*_{k,\mp k'}Q^\dagger_{k,\pm k'}$, switch $f_\uparrow$ with $f_\downarrow$, and $\pm k'$ with k. The minus sign from commutation can be absorbed into $h_{k,k'}=-h_{k',k}$. The total change is switching $g_{k,-k'}(m'-n')$ with $g^*_{k',-k}(n-m)^*$, keeping the dirac deltas same.

$$\begin{aligned}\Sigma^n_{\downarrow\downarrow}(k) = \tfrac{-1}{\beta}\sum_{k',p}\Big(&2G^f_{\uparrow\uparrow}(k')G^\Gamma_r(q)\cdot|g_{k',k}|^2|w_{3r,q}-z_{3r,q}|^2\cdot\left(\delta_{q+k'-k}+\delta_{q+k-k'}\right)\\&+G^f_{\downarrow\downarrow}(k')G^\Gamma_r(q)\cdot|g_{k',-k}|^2\left(|n_{r,q}-m_{r,q}|^2\delta_{q+k-k'}+|m'_{r,q}-n'_{r,q}|^2\delta_{q+k'-k}\right)\\&-G^f_{\downarrow\downarrow}(k')G^\Gamma_r(q)\cdot|h_{k,-k'}|^2|w_{3r,q}-z_{3r,q}|^2\cdot\left(\delta_{q+k+k'}+\delta_{q-k-k'}\right)\Big)\\&+g_{k,k}(\Xi_Q+\Theta^Q_{q,r}\cdot G^\Gamma_r(q))\end{aligned} \tag{A.9}$$

$$\begin{aligned}\Sigma^a_{\downarrow\downarrow}(k) = \tfrac{-1}{\beta}\sum_{k',p}\Big(&G^f_{\downarrow\downarrow}(k')G^\Gamma_r(q)\cdot g_{k',-k}h^*_{k,k'}\big((n_{r,q}-m_{r,q})(iz_{3r,q}-iw_{3r,q})^*\cdot\delta_{q+k-k'}\\&+(m'_{r,q}-n'_{r,q})(iz_{3r,q}-iw_{3r,q})\cdot\delta_{q+k'-k}\big)\\&-G^f_{\downarrow\downarrow}(k')G^\Gamma_r(q)\cdot g_{-k',k}h^*_{-k,-k'}\big((n_{r,q}-m_{r,q})(iz_{3r,q}-iw_{3r,q})^*\cdot\delta_{q-k-k'}\\&+(m'_{r,q}-n'_{r,q})(iz_{3r,q}-iw_{3r,q})\cdot\delta_{q+k'+k}\big)\Big)\end{aligned} \tag{A.10}$$

Next we perform the matsubara summation. The general form of summations in self energies is,

$$\tfrac{1}{\beta}\sum_{ik'_n,iq_n}G^f(k',ik'_n)G^\Gamma(q,iq_n)\delta_{\sigma ik_n+\sigma' ik'_n-iq_n}=\tfrac{1}{\beta}\sum_{ik'_n}\frac{1}{ik'_n-E^f_{k'}}\frac{1}{\sigma ik_n+\sigma' ik'_n-E^\Gamma_q}.$$

Since this a fermionic frequency summation, the above would equal,

$$\sum_{z_j} \mathrm{Res}\left[\frac{1}{z-E^f_{k'}}\frac{1}{\sigma ik_n+\sigma' z-E^\Gamma_q}\right] n_F(z_j)$$
$$=\frac{n_F(E^f_{k'})}{\sigma ik_n+\sigma' E^f_{k'}-E^\Gamma_q}+\frac{-\sigma' n_B(\sigma' E^\Gamma_q)}{\sigma' E^\Gamma_q-\sigma'\sigma ik_n-E^f_{k'}}=\frac{n_F(E^f_{k'})+n_B(\sigma' E^\Gamma_q)}{\sigma ik_n+\sigma' E^f_{k'}-E^\Gamma_q}.$$

Finally note that $n_{F/B}(E)=0$ if $E>0$. Since both fermionic and triplon energies are positive, the only surviving terms will be the ones where $q=-k'\pm k$. An s-wave gap function lends further simplification, since u_k and v_k are then even functions of k,

$$\therefore g_{k',k}=g_{k',-k}=g_{k,k'},\quad h_{k',k}=h_{k',-k}=-h_{k,k'}.$$

Appendix B

Spin-ladder at zero magnetic field

To start, we re-write the reduced form of $h_y = 0$ triplon hamiltonian in Eq.(3.21) in a manner to highlight the main features,

$$h(k) = \begin{pmatrix} h_1(k) & h_2(k) \\ h_2^\dagger(k) & h_1(k) \end{pmatrix}; \quad \begin{matrix} h_1(k) = a_1(k)\mathbb{I} + \mathbf{d}\cdot\mathbf{Z}; \\ h_2(k) = a_2(k)\mathbb{I} - \mathbf{d}\cdot\mathbf{Z} \end{matrix}$$

where $d = (\Gamma\cos(k), -D\sin(k), 0)$, and $\mathbf{Z}$ is set of matrices from representation of $\mathfrak{su}(2)$. Notice, h_1 and h_2 are same upto identity, hence they commute. This greatly simplifies the problem, since both are now diagonalized by the same unitary matrix.

$$M_k^a = \frac{1}{|d_k|\sqrt{2}} \begin{pmatrix} |d_k| & 0 & -\Gamma\cos(k) - iD\sin(k) \\ 0 & 1 & 0 \\ \Gamma\cos(k) - iD\sin(k) & 0 & |d_k| \end{pmatrix},$$

$$M_k^b = \frac{1}{|d_k|\sqrt{2}} \begin{pmatrix} |d_k| & 0 & |d_k| \\ \Gamma\cos(k) & -iD\sin(k) & -\Gamma\cos(k) \\ -iD\sin(k) & \Gamma\cos(k) & iD\sin(k) \end{pmatrix},$$

where, M_k^a and M_k^b are matrices that diagonalize $h_{1,2}(k)$ for the case $\mathbf{Z} = \sigma$ in Eq.(2.2) and $\mathbf{Z} = \mathbf{L}$ in Eq.(2.5), respectively.

To get the BdG coefficients we diagonalize $\Sigma h(k)$, where $\Sigma = \mathrm{Diag}(\mathbb{I}, -\mathbb{I})$. The required unitary matrix can be deduced as follows, first diagonalize the blocks,

$$\mathbb{I}_2 \otimes M_k^\dagger \cdot \Sigma h(k) \cdot \mathbb{I}_2 \otimes M_k = \begin{pmatrix} E_{h_1}(k) & E_{h_2}(k) \\ -E_{h_2}(k) & -E_{h_1}(k) \end{pmatrix}$$

where, $E_{h_i}(k)$ is diagonal containing eigenvalues of h_i. Next we diagonalized the above matrix into the form $\mathrm{Diag}(E(k), -E(k))$ where, $E(k) = \sqrt{|E_{h_1}(k)|^2 - |E_{h_2}(k)|^2}$. The required unitary is,

$$N_k = \begin{pmatrix} \alpha_+ & \alpha_- \\ -\alpha_- & -\alpha_+ \end{pmatrix}, \quad [\alpha_\pm]_{ii} = \mathrm{sgn}([E_{h_2}]_{ii}) \left(\frac{[E_{h_1}]_{ii} \pm [E]_{ii}}{2\,[E]_{ii}} \right)^{1/2}$$

In the above expression we have dropped k variable. The total unitary is therefore $\mathbb{I}_2 \otimes M_k \cdot N_k$, which on comparison with Eq.(3.6) gives the W_k and Z_k coefficients,

$$\mathbb{I}_2 \otimes M_k \cdot N_k = \begin{pmatrix} M_k\alpha_+ & M_k\alpha_- \\ -M_k\alpha_- & -M_k\alpha_+ \end{pmatrix} \quad \Rightarrow \quad \begin{matrix} W_k = M_k\alpha_+ \\ Z_k = -M_{-k}\alpha_- \end{matrix}$$